World Journal of Advanced Research and Reviews
eISSN: 2581-9615 CODEN (USA): WJARAI
Cross Ref DOI: 10.30574/wjarr
Journal homepage: https://wjarr.com/

(RESEARCH ARTICLE)

Check for updates

Physico-chemical, mineralogical and structural characterization of a clay of Tanout (Zinder-Niger)

Rabilou Souley Moussa [1, *], Zeinabou Mahamadou [1], Ousmaila Sanda Mamane [2], Issa Habou [3], Maman Mousbahou Malam Alma [1] and Ibrahim Natatou [1]

[1] *Materials, Water and Environment Laboratory (LAMEE), Faculty of Science and Technology, Abdou Moumouni University of Niamey, B.P :10662 Niamey, Niger.*
[2] *Department of chemistry, Faculty of Science and Technology, University of Agadez, B.P: 199 Agadez, Niger.*
[3] *Water Analysis Laboratory Regional Direction of Hydraulics and Sanitation of Zinder, B.P: 480, Niger.*

World Journal of Advanced Research and Reviews, 2022, 16(02), 1077–1092

Publication history: Received on 14 October 2022; revised on 24 November 2022; accepted on 26 November 2022

Article DOI: https://doi.org/10.30574/wjarr.2022.16.2.1272

Abstract

The objective of this study is to identify the different mineral phases, the structural and textural properties of natural clay of Tanout in Zinder region (Niger) in order to have mineralogical data allowing its valuation. The methodology is based on a physicochemical characterization by coupling several analysis techniques (preliminary analyses, X-ray fluorescence, X-ray diffraction, thermos- gravimetric analysis, scanning electron microscopy, Brunauer-Emmett-Teller by adsorption of N_2 at 77 K). The results from these analyzes show that this clay has a low humidity rate, a low density, a slightly neutral pH in an aqueous medium and a high cation exchange capacity and is mainly composed of SiO_2 (68.1%), Al_2O_3 (17.02%) and Fe_2O_3 (7.6%) with trace elements, the most important of which are: Zr (4150.6 ppm), Sr (470 ppm), Cu (380.2 ppm) and V (320ppm). It essentially consists of Kaolinite and Montmorillonite with impurities such as quartz and microclines. It has a specific surface of 441.1 $m^2.g^{-1}$ and 2288 $m^2.g^{-1}$ calculated according to the BET and Langmuir methods respectively, with porous volume varying from 0.0157 to 0.2597 $cm^3.g^{-1}$ and of pore size which varies from 1.847 to 6.182 nm calculated according to the methods (Barrett-Joyner-Halenda, Dubinin-Radushkevich, Dubinin-A, Horvath-Kawazoe and Saito-Foley). This clay has an important degree of crystallinity. These characteristics make it a potential material that can be used in water pollution control.

Keywords: Natural clay; Characterization; Mineralogical data; Crystallinity; Tanout; Zinder; Niger

1. Introduction

In recent years, many porous materials have been developed for the treatment of water intended for consumption because of their deterioration. Some of them were effective but very expensive, polluting and inapplicable in rural areas. Economic constraints and environmental concerns have aroused scientific interest in the search for materials of natural origin [1], which are inexpensive, less polluting and easily accessible, in this case clay materials. Numerous research works have shown the anti-polluting role of clay materials due to their physico-chemical, mineralogical, structural and textural properties [2]. However, in Niger, this field of research remains in embryonic state, where uniquely the only studies carried out to eliminate fluoride ions by bentonite from Niger [3] and the elimination of copper from consuming water by two clay materials from the Niger River valley [4]. We also note the studies on the characterization of clays used in pottery such as that carried out in Mirriah of Zinder region [5], that carried out in Djirataoua in Maradi region [6] and the characterization of a mixed clay of Tahoua region [7]. With a view to enhancing natural resources in Niger, a clay of Tanout department of Zinder region was characterized by combining several analysis techniques (X-ray

* Corresponding author: Rabilou Souley Moussa
Materials, Water and Environment Laboratory (LAMEE), Faculty of Science and Technology, Abdou Moumouni University of Niamey, B.P :10662 Niamey, Niger.

fluorescence, X-ray diffraction; Thermogravimetric analysis, scanning electron microscopy, BET by adsorption of dinitrogen at 77 K) whose objective is to identify the different mineral phases, the textural and structural properties in order to have mineralogical data allowing its use in the depollution of water. To our knowledge, this clay material has not been the subject of work devoted to characterization from a mineralogical, physico-chemical and textural point of view.

2. Material and methods

2.1. Presentation of clay sampling site

The clay sample used in this study was taken from a quarry located in west of the town of Tanout (Zinder). From the geological point of view, this clay belongs to a clayey to silty formation of the upper marine Cretaceous, which, except for a few discontinuous parts of sand, does not contain water. This clay formation outcrops on the mountain of Zozowa and the hills of Gangara and Tanout. In the township of Tanout, it reaches a thickness of 300 m. Figure 1 and Table 1 present respectively the sampled site and the geographical coordinates with the nomenclature of the sample. After drying at room temperature, this sample was sent to the Materials-Water and Environment Analysis Laboratory (MWEAL) of Abdou Moumouni University (AMU) for preliminary processing and purification.

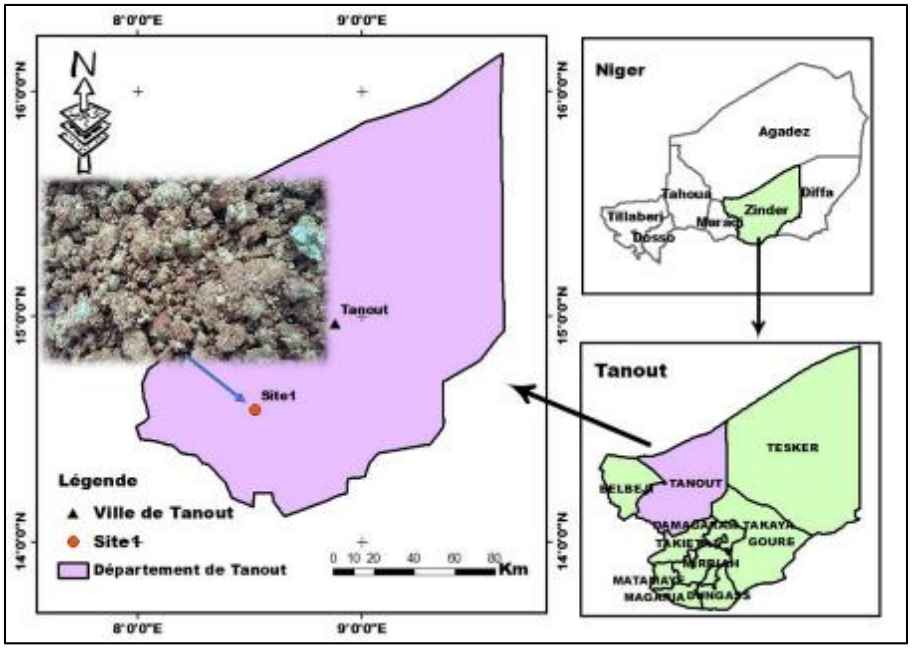

Figure 1 Representation of the natural clay sampling site

Table 1 Geographical coordinates of the site and nomenclature of the sample

Site	Longitude	Latitude	Name of sample
Site 1	08.52590	14.58261	Arg1-B

2.2. Preliminary processing

The raw clay samples were crushed, then ground using a jaw crusher and sieved using a 200 µm grain size sieve. This step eliminates a number of impurities such as quartz and reduces the sample to millimetric fragments. These operations were carried out at the Second Year Chemistry Laboratory (SYCL) of the AMU.

2.3. Purification of the raw clay (extraction of the clay fraction < 2 µm)

This technique removes accessory minerals (quartz, carbonates, feldspar, etc.) and extracts the fine fraction rich in clay minerals. The protocol used was developed by M. Robert and D. Tessier in [8]. Figure 2 presents the experimental device used. The clay fractions obtained were named Arg1-FNa$^+$ and Arg1-FSNa$^+$.

Figure 2 Communicating vessel system for the extraction of the fraction < 2 µm

2.4. Humidity rate

The evaluation of the moisture content can be indicative of the hydrophilic behavior of adsorbent materials. The method consists of weighing the empty crucible, noting the weight P, then the hollowed one containing 2 g of clay, noting the weight P1. The assembly was brought to an oven at 105°C for 24 hours, then cooled in a desiccator for 30 min while again weighing the weight P2. The moisture content was calculated by the following formula [9].

$$H\ (\%) = \frac{P_1 - P_2}{P_1 - P}\ x\ 100\ (1)$$

2.5. Density

Density is the set of solid and pore fractions. It was determined by the test tube method. This density was calculated by the following formula:

$$\rho\ (g.cm^{-3}) = \frac{P_2 - P_1}{V}(2).$$

2.6. Raw clay pH

The determination of the pH is necessary to quantify the contribution of the acidity when the solid is in contact with the solution. 1g of clay was put in contact with 100 ml of distilled water under magnetic stirring at room temperature for 2 hours. The pH was measured after filtration. To verify the effect of the mass of clays on the pH, increasing masses of clays (1, 3 and 5 g) were brought into contact with 50 ml of distilled water under magnetic stirring at room temperature, then the mixture was allowed to stand for 24 hours. Finally, the pH of Arg1-B was measured *AFNOR in* [10].

2.7. Cation exchange capacity (CEC) by conductimetry

The cation exchange capacity was determined by the conductimetric method [10, 11]. It consists of putting 1 g of clay in 100 ml of distilled water under magnetic stirring at room temperature for 2h 30'. After adding 150 ml of a 1 M $BaCl_2$ solution while adjusting the pH to that of the raw clay, the suspension was left under stirring for 2h 30'. Then the suspension was filtered and washed to a negative $AgNO_3$ test, then oven-dried overnight at 60°C. After grinding, 0.5 g of treated clay was brought into contact with 50 ml of distilled water under magnetic stirring at room temperature for 2 hours followed by conductimetric titration with a 0.02 M $MgSO_4$ solution. At each addition of 0.5 ml of $MgSO_4$ solution, the conductivity value was noted after stabilization. Finally, the curve of conductivity as a function of the volume of $MgSO_4$ poured was plotted and the equivalent point which corresponds to the intersection of two half-lines tangent to the curve was determined. The CEC was calculated by the following formula:

$$CEC\ (méq.100g^{-1}) = 2C\ x\ \frac{V}{m}\ x\ 100\ (3).$$

2.8. Loss on ignition (LOI)

The same clay sample was subsequently heated at 1000°C for 2 hours to determine the LOI. The latter was determined gravimetrically by heating 1 g of powdered clays in a cleaned weighed crucible to 1000°C. After which, the crucible and the contents were weighed to obtain the difference in weight before and after heating. The following formula was applied to determine the LOI.

$$LOI = \left(\frac{a-b}{a}\right) x\ 100 \quad (4)$$

With: a = weight of the crucible + 1 g of the sample before heating, b = weight of the crucible + 1 g of the sample after heating. The analysis was carried out at the National Geoscience Research Laboratories (NGRL) in Kaduna (Federal Republic of Nigeria).

2.9. Isoelectric point or pH at point of zero charge (pH_{PCN})

The isoelectric point or pH_{PCN} corresponds to the pH value for which the net charge of the solid surface is zero. This method consists of putting 50 mg of clays in 50 ml of distilled water with a pH between 2 and 12 (adjusted by solutions of HCl and 0.01M NaOH) with magnetic stirring at room temperature for 24 hours. Afterwards, the final pH of the suspension was measured and the graph pHf – pHi as a function of pHi was drawn. The isoelectric point corresponds to the intersection of the curve and the straight line which passes through the origin [12]. This parameter was determined for the raw sample and the clay fractions < 2 µm.

2.10. X-ray fluorescence spectrometry (XRF)

As part of this work, an energy dispersive X-ray fluorescence spectrometer (EDXRF) of the "Minipal 4" model was used for the analysis of Arg1-B, Arg1-FNa^+ and Arg1-$FSNa^+$ available to Kaduna NGRL.

2.11. X-ray diffraction (XRD)

In this study, an Empyrean diffractometer DY674 (2010) with copper anode manufactured by Panalytical (Holland) was used for the determination of the mineralogical composition of raw clay and clay fractions < 2 µm at the Kaduna NGRL. The condition for the radiations to be in phase is expressed by Bragg's law: $n\lambda=2d_{hkl}\ \sin\theta$ (5). In the tube, the current was 40 mA and the voltage was 45 kV. The ICDD (International Center for Diffraction Data) PDF (Powder Diffraction File) 4 (2015) and COD (2016) databases make it easy to find and match the diffractogram to identify mineral phases and compounds.

2.12. Thermo-gravimetric Analysis (TGA)

The device used in this study is of the PerkinElmer MES-TGA TGA4000 brand, manufactured in the Netherlands. This clay was subjected to a temperature range from 28.13°C to 950°C with a constant rate of 10°C per min under a nitrogen flow. The analysis was carried out at the Block B Multipurpose Laboratory of the Federal University of Technology, Mina (Federal Republic of Nigeria).

2.13. Scanning electron microscopy (SEM)

In this study, the morphology of the raw clay sample and clay fractions was observed using a Phenom ProX type scanning electron microscope at the Laboratory of the Department of Engineering Chemistry of Ahmadu Bello University (ABU) of Zaria (Federal Republic of Nigeria). In an experimental way, the samples were placed on a double adhesive tape, then sprayed. Afterwards, they were deposited in a sputter coater (quorum-Q150R Plus E) with 5 nm gold.

2.14. Measurement of SS by the Brunauer, Emmett and Teller (BET) method

In addition to the thermo-gravimetric analyses, it is quite conclusive to evaluate the SS, the pore volumes and the microporous sizes of our clay sample. Because it is the quality and extent of these surfaces that will largely determine the adsorption capacities of this clay material. The SS of this clay material was determined at the Block B Multipurpose Laboratory of the Federal University of Technology, Mina (Federal Republic of Nigeria). These measurements were taken using a Quanta-chrome Nova 4200e device manufactured in the United States.

3. Results

3.1. Preliminary analyzes of raw clay (Arg1-B)

The results of the preliminary analysis (density, moisture content, pH and CEC) are presented in Table 2.

Table 2 Results of preliminary analyzes of the raw sample

Clay	H (%)	ρ (g.cm-3)	pH	CEC (méq.100 g-1)
Arg1-B	1.995	1.184	6.665	124.24

The analysis of this table shows that, this clay has a low humidity rate and a low density with a slightly neutral pH in an aqueous medium. However, the increase in the mass of this clay leads to a regression of this pH (Figure 3). It has a high CEC of the order of 124.24 meq.100 g^{-1}. This CEC, which is the number of cations that can be substituted for the compensating cations to compensate for the negative charge of 100 g of clay, varies according to the materials.

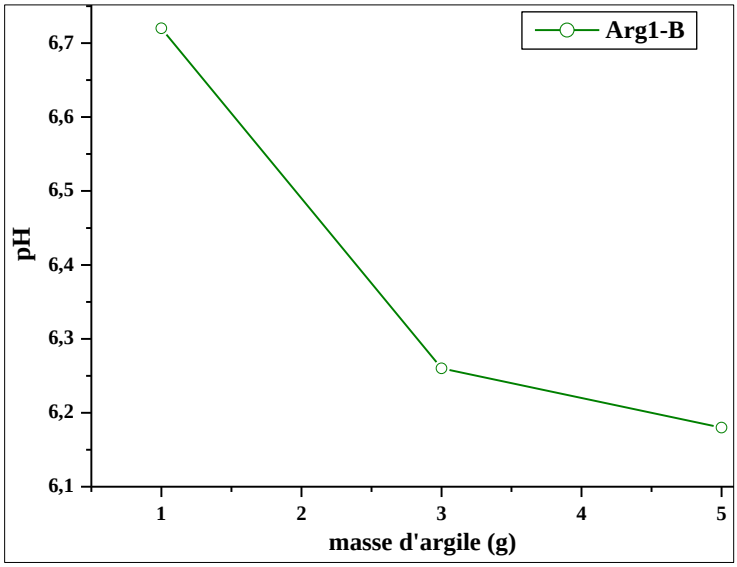

Figure 3 Variation in the pH of raw clays as a function of mass

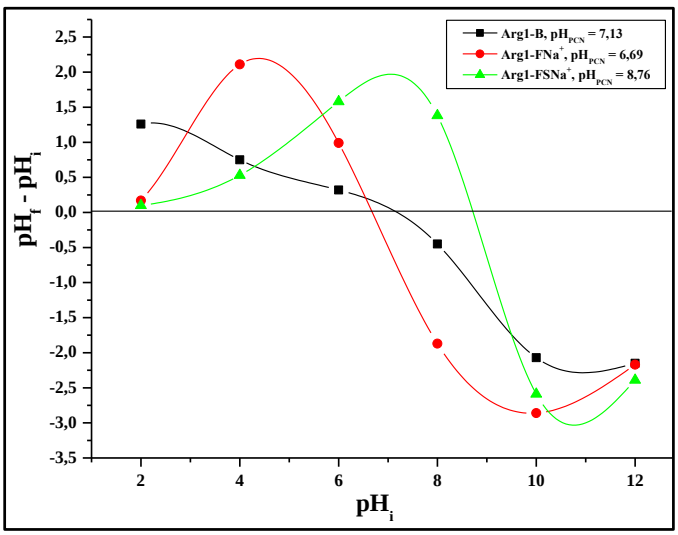

Figure 4 pH_{PCN} of raw clay and clay fractions

The figure below (Figure 4) presents the different values of pH_{PCN} or isoelectric point of the raw clay sample and the clay fractions. These values are 7.13 for the raw clay, 8.76 for the clay fraction without Na^+ and 6.69 for the soda clay fraction. Overall, there is an increase in pH_{PCN} of the clay fraction without Na^+ compared to that of the raw sample and a decrease in pH_{PCN} for the sodium clay fraction. These isoelectric points characterize the acidity or the alkalinity of the surface of the studied material and they are very important factors in the phenomenon of sorption especially when the electrostatic forces are involved in the mechanism of adsorption. So for pH values lower than the pH_{PCN} found in this study, the surface charge of these clays is positive, when they are higher it becomes negative and when they are equal the charges balance out, so the surface becomes electrically neutral (there is as much positive as negative charge).

3.2. X-ray fluorescence spectrometry (XRF)

The results of X-ray fluorescence analysis of the raw clay sample and the clay fractions are recorded in Table 3 for the major oxides and the loss on ignition and in Table 4 for the trace elements.

Table 3 Percentages of major oxides of raw clay and clay fractions and those of the loss on ignition

Oxides (%)	Arg1-B	Arg1-FSNa$^+$	Arg1-FNa$^+$
SiO_2	68.1	51.25	50.5
Al_2O_3	17.02	24.51	26.8
K_2O	2	0.7	0.4
Na_2O	0.82	0.07	0.1
CaO	0.2	0.09	0.18
MgO	0.23	0.002	0.024
TiO_2	1.62	1.25	1.2
MnO	0.048	0029	0.035
P_2O_5	0.002	0.001	ND
SO_3	0.14	ND	0.001
Fe_2O_3	7.6	4.11	4.01
PAF	0.98	16.4	16.4
SiO_2/Al_2O_3	4.001	2.09	1.884

Table 3 shows the following observations:

- In raw clay (Arg1-B) silica and alumina are the major constituent oxides. The percentage of silica in this clay exceeds 50%. This leads to a SiO_2/Al_2O_3 ratio equal to 4.001.
- This raw clay contains a fairly large percentage of iron oxide (Fe_2O_3).
- It should also be noted the presence of K_2O and TiO_2 in significant quantities in this clay.
- The low percentages of CaO and MgO show that, this clay contains slightly carbonates of calcium and magnesium.
- The low percentages of $Na_2O < 1\%$ show that this clay contains a negligible quantity of alkaline feldspars.
- The LOI, which is likely to estimate the rate of organic matter and carbonates contained in this clay, shows that it has a value of less than 1%.
- For the clay fractions (Arg1-FSNa$^+$, Arg1-FNa$^+$), the silica percentages decrease compared to that of the raw clay. In addition, the Al_2O_3 percentages of these clay fractions exceed that of the raw clay. This shows that, this clay is becoming more and more aluminous. Contrary to the percentages in Fe_2O_3 which decrease compared to that of the raw clay, but, their percentages in LOI largely exceed that of the raw clay.

Table 4 Trace element of raw clay and clay fractions in ppm

Elements of trace	Arg1-B	Arg1-FSNa⁺	Arg1-FNa⁺
V	320	230	200.2
Cr	80.21	160.21	170
Ni	<0.001	<0.001	<0.001
Zn	120	200.44	200.22
Cu	380.2	280	260
Ga	ND	7.748	67
Sr	470	420	430.11
Y	5.4	5.6	5.8
Zr	4150.6	410.241	420
Hf	61.034	13.38	62.03
Ba	<0.001	1000	1000
Ce	11.7	60.24	7.8
Eu	0.234	0.17	1.9
Re	0.031	0.022	0.02
Pb	48	ND	100

- ND: not detected

The analysis of Table 4 shows us that the raw clay used in this study presents trace elements such as: V, Cr, Zn, Cu, Sr, Zr, Hf, Ce and Pb in ppm. Zr is the most abundant trace element, followed by Sr, then V, Cu, Zn and Cr. But, in the clay fractions, the percentages of the aforementioned elements decrease, except those of Zn, Cr, which increase and especially for Ba which goes from about 0.001 ppm to 1000 ppm in the raw clay.

3.3. X-ray diffraction (XRD)

The results of the mineralogical analyzes carried out on the raw clay and the clay fractions by X-ray diffraction are given in the figures below. These figures, after indexing the set of peaks of each phase by the ICDD and COD database, show the following observations:

Arg1-B consists of Kaolinite (K), Montmorillonite (M), microclines (Mc) and quartz (Q). The characteristic peaks of Kaolinite at 2θ = 12.39°, 20.36°, 24.94°, 36.06°, 38.32°, 38.52°, 39.37°, 41.14°, 42 .41°, 45.67°, 49.48°, 51.18°, 54.94°, 60.37°, 62.28°, 63.83°, 64.77°, 65.84° and 68 .35° correspond respectively to the reticular distances 7.13 Å, 4.35 Å, 3.56 Å, 2.48 Å, 2.34 Å, 2.33 Å, 2.28 Å, 2.19 Å, 2, 12Å, 1.98Å, 1.84Å, 1.78Å, 1.66Å, 1.53Å, 1.48Å, 1.45Å, 1.43Å, 1.41Å and 1, 37 Å (file: 96-900-9235). The chemical formula of this kaolinite is $Al_2Si_2O_9H_4$. As for montmorillonite, it is characterized by peaks at 2θ = 9.12°, 19.8°, 21.13°, 27.6°, 35.47°, 36.46°, 40.42°, 46 ,13°, 55.87°, 59.14°, 62.12°, 62.42°, 64.21°, 67.66°, 68.73° correspond respectively to lattice distances 9.68 Å, 4, 47Å, 4.2Å, 3.22Å, 2.52Å, 2.46Å, 2.33Å, 2.22Å, 1.96Å, 1.64Å, 1.56Å, 1, 49Å, 1.48Å, 1.44Å, 1.38Å, 1.36Å (file: 96-901-0959). This montmorillonite has the chemical formula $Si_{7.8}Al_{1.72}Li_{0.16}Fe_{0.20}Mg_{0.28}O_{20}$. The peaks of the microclines are observable at 2θ = 13.12°, 21.6°, 24.72°, 25.52°, 25.66°, 27.07°, 27.38°, 27.52°, 35 .55°, 39.96°, 40.52°, 41.53°, 45.48°, 47.14°, 50.52°, 55.53°, 56.01°, 59.90° respectively at lattice distances 6.74 Å, 4.22 Å, 3.7 Å, 3.48 Å, 3.46 Å, 3.36 Å, 3.29 Å, 3.25 Å, 3.24 Å, 2, 52Å, 2.29Å, 2.22Å, 2.16Å, 1.99Å, 1.92Å, 1.80Å, 1.65Å, 1.64Å, 1.54Å (File: 96-900-4192). Their chemical formula is $K_{1.9}Na_{0.1}Al_2Si_6O_{16}$. Quartz peaks are noticeable at 2θ = 20.85°, 26.63°, 36.54°, 39.46°, 40.28°, 42.44°, 45.79°, 50.13°, 54 ,86°, 55.32°, 59.95°, 64.02°, 67.73° and 68.13° corresponding respectively to the reticular distances 4.25 Å, 3.34 Å, 2.45 Å, 2, 28Å, 2.23Å, 2.12Å, 1.98Å, 1.81Å, 1.67Å, 1.65Å, 1.54Å, 1.45Å, 1.38Å and 1, 37 Å (file: 96-901-2601). This quartz has the chemical formula Si_3O_6.

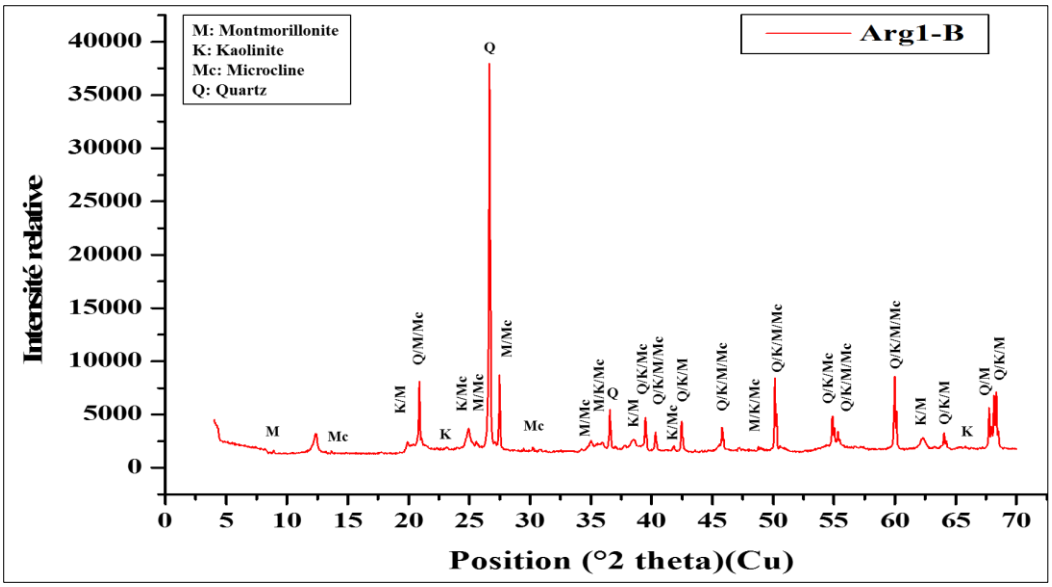

Figure 5 Diffractogram of Arg1-B

Arg1-FSNa⁺ presents intense peaks characteristic of kaolinite and montmorillonite with disappearance of peaks characteristic of microclines and appearance of peaks characteristic of goethite. The characteristic peaks of quartz remain, but with low intensities compared to the raw state. The characteristic peaks of these minerals apart from goethite have already been detailed above in point Arg1-B, but, for goethite, they appear at 2θ = 21.27°, 26.38°, 33.30°, 34.74°, 36.11°, 36.72°, 39.15°, 40.23°, 45.13°, 48.13°, 49.94°, 50.71° and 68.62°, which correspond respectively to the reticular distances 4.16 Å, 3.34 Å, 2.67 Å, 2.56 Å, 2.49 Å, 2.45 Å, 2.28 Å, 2.23 Å, 1.99 Å, 1.895 Å, 1.81 Å, 1.78 Å and 1.37 Å (file: 96-901-0409). This goethite has the chemical formula $Fe_{3.8}Co_{0.2}O_8$ and it crystallizes in the orthorhombic system.

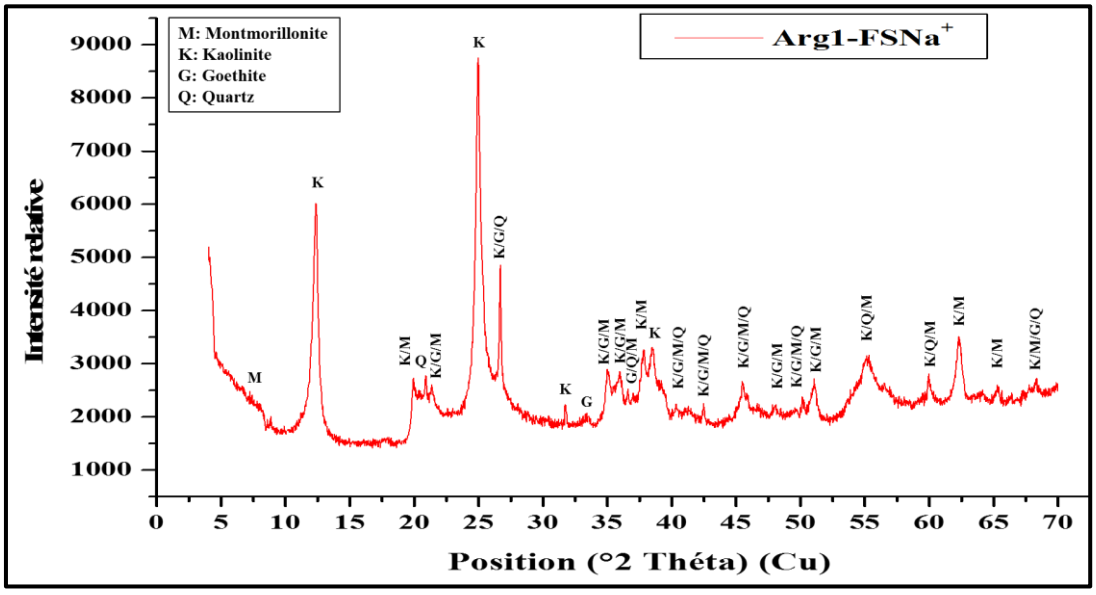

Figure 6 Diffractogram of Arg1-FSNa⁺

Arg1-FNa⁺ homoinic sodium retains the same minerals as before, but with much more intense peaks. So homoionization with sodium increases the intensity of the characteristic peaks of the minerals that make up this clay.

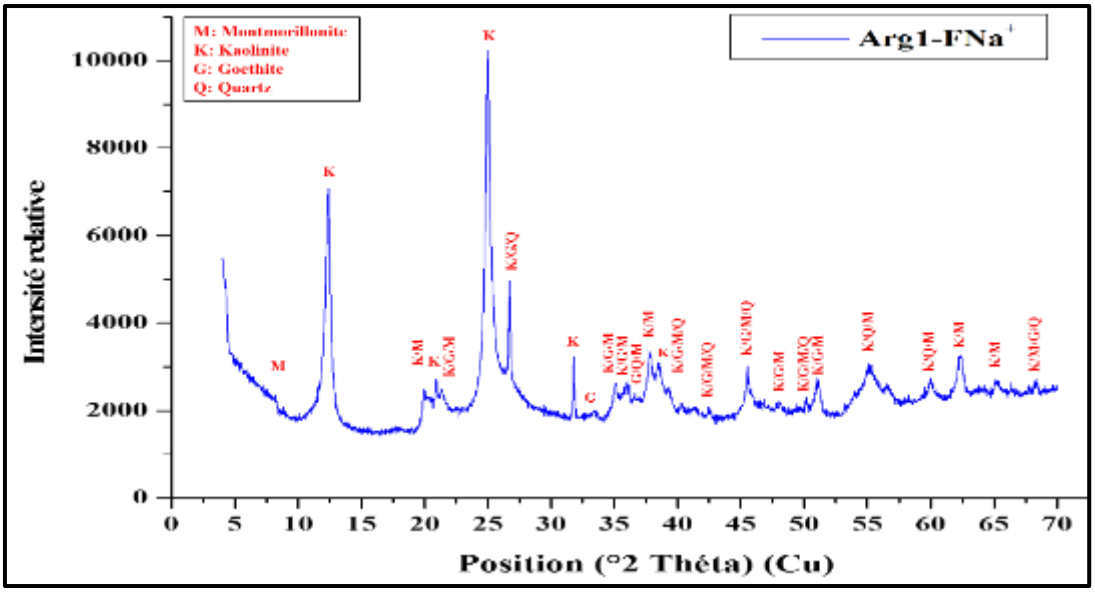

Figure 7 Diffractogram of Arg1-FNa⁺

3.4. Thermo-gravimetric Analysis (TGA)

The result of the thermo-gravimetric analysis carried out on the raw clay is presented in Figure 8.

The analysis of Figure 8 shows that the TGA curve presents five mass losses at different temperatures. The first is observable from 28.13 to 152.76°C causing a loss of 3.926%, the second largest is observable from 168.48 to 363.69°C with a loss of 60.674%, the third is remarkable from 363.69 to 428.05°C causing a loss of 22.281%, the fourth is noticeable from 428.05 to 695.03°C causing a loss of 7.454% and the last from 695.03 to 704.77°C with a loss of 1.086%. The figure also shows two small increases in weight in the ranges 152.76 to 168.48°C and 704.77 to 788.06°C. The derivative of the TGA curve (DTG) shows four endothermic peaks (at 147.23°C, 336.76°C, 406.71°C and 699.87°C) and two exothermic peaks (at 157. 46°C and 708.19°C).

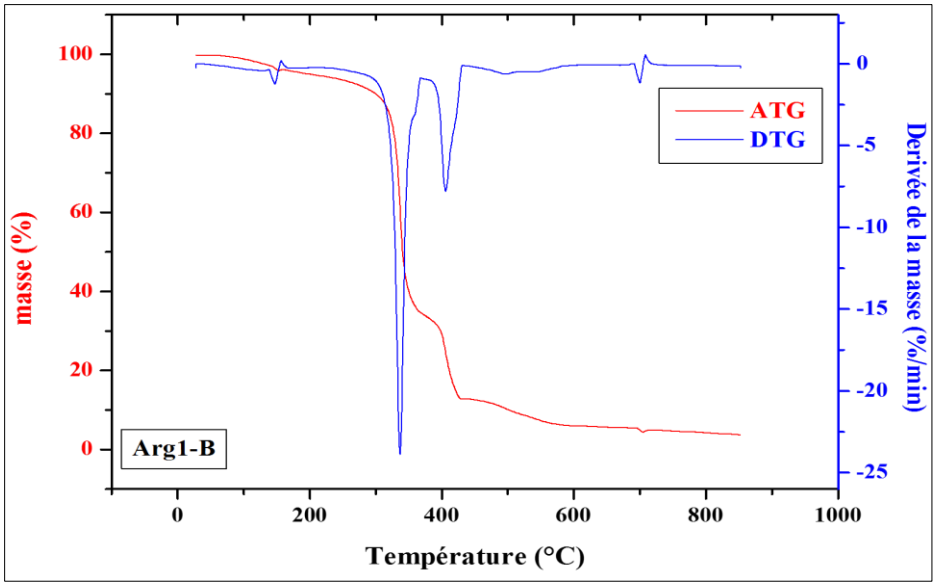

Figure 8 TGA and DTG curve of Arg1-B

3.5. Scanning electron microscopy (SEM)

SEM was used to observe the morphology and organization of clay particle aggregates. The images obtained from the raw clay and the clay fractions are shown in Figure 9. The micrographs show that, this clay has morphologies showing

crystals of irregular shape distributed in a random manner. The clay fraction without Na^+ (Arg1-$FSNa^+$) does not show a big difference with the morphology observed in the raw state, but, its sodium homoionic fraction (Arg1-FNa^+), shows an agglomeration of these crystals forming a compact mass. Given the diversity of minerals identified contained in these clay particles by XRD and the low resolution of the SEM image of this clay, the structural identification of the morphologies specific to the basic clay minerals (Kaolinite, montmorillonite) remains very difficult. But, it shows the degree of crystallinity of this clayey material.

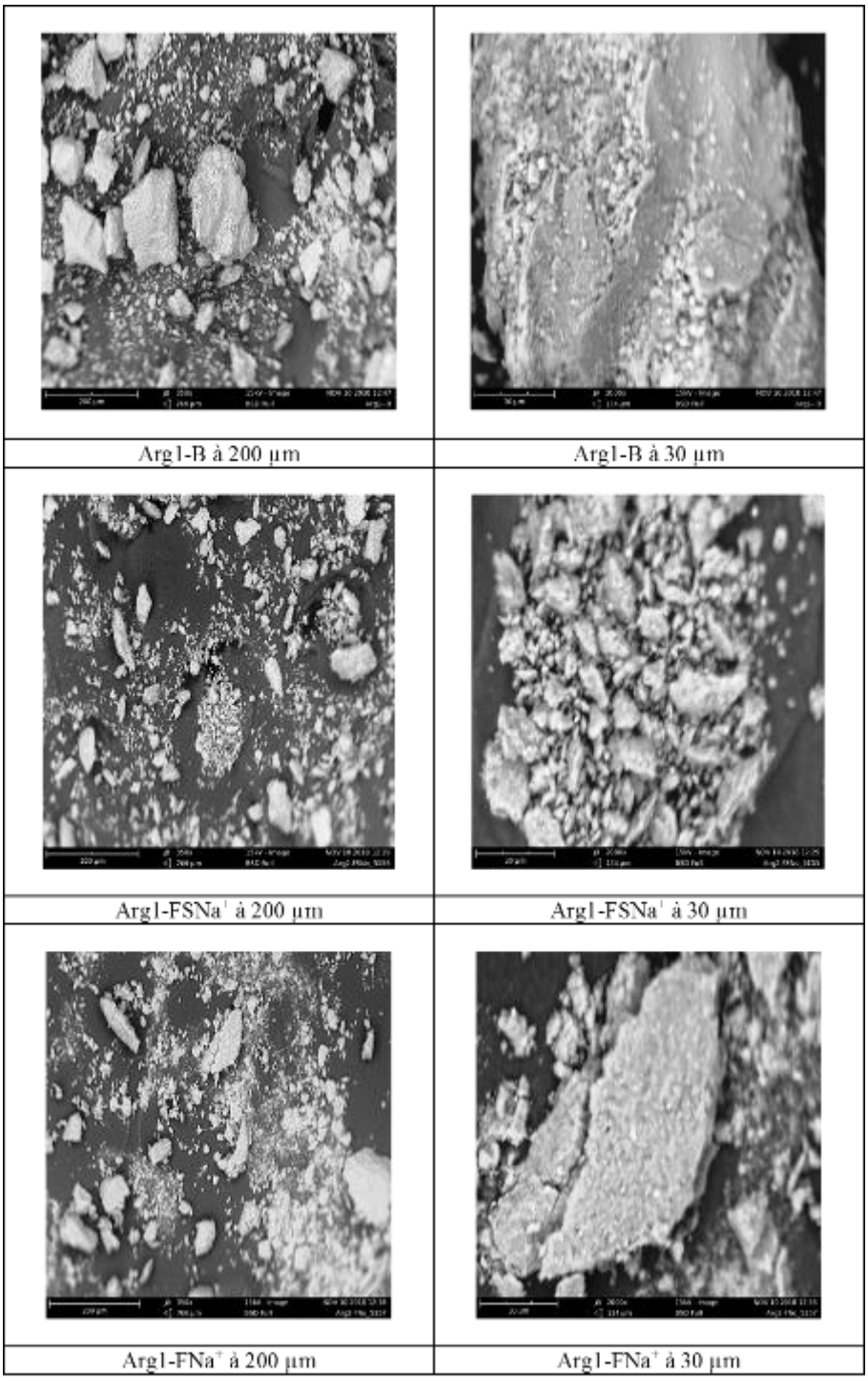

Figure 9 SEM images of Arg1-B, Arg1-$FSNa^+$ and Arg1-FNa^+

3.6. Measurement of SS by the Brunauer, Emmett and Teller (BET) method

The SS of the clay calculated according to the methods are recorded in Table 5.

Table 5 Different surfaces of raw clay

Characteristic	Sizes	Arg1-B
Specific surface ($m^2.g^{-1}$)	at P/P0 = 0.3	278.8
	BET	444.1
	Langmuir	2288
	Cumulative (BJH)	514.4
	Cumulative (DH)	548.4
	External (t-method)	444.1
	Micropores (DR)	485.9
	Cumulative (DFT)	109

This table shows that the SS vary according to the methods used. At one point (P/P0 = 0.3), Arg1-B exhibits a significant SS, but it is lower than that found by BET. A very impressive value was obtained by the Langmuir method of around 2288 $m^2.g^{-1}$. Regarding the cumulative SS according to the methods (BJH and DH), the difference is not significant, but it moderately exceeds that of BET and remains below that of Langmuir. The external SS determined by t-method is similar to that of BET, while the microporous one determined by DR method slightly exceeds it. As for the DFT method, it shows SS values that are below the values found for the other methods.

These SS obtained by the different methods show that these clays are potential candidates for adsorption.

The results of the pore volumes of the raw clay calculated according to the different methods are recorded in the following table:

Table 6 Pore volumes of raw clay

Characteristic	Sizes	Arg1-B
Volume ($cm^3.g^{-1}$)	BJH (cumulative)	0.2536
	DH (cumulative)	0.2597
	DR (micropore)	0.1727
	HK (micropore)	0.073
	SF (micro-pore)	0.0157
	DFT (cumulative)	0.1314

The analysis of this table shows that the cumulative pore volumes according to the BJH and DH methods do not show a significant difference, but they greatly exceed that calculated according to the DFT method. While the micro-pore volumes according to pore shapes by HK and SF methods show significant difference. That of HK (0.073 $cm^3.g^{-1}$) corresponding to the slit-like shape is much higher than that of SF (0.0157 $cm^3.g^{-1}$) corresponding to the cylindrical-like shape. But, they are lower than that calculated according to the DR method.

The results of the pore size distribution calculated according to the different methods are presented in the following table:

Table 7 Pore size of raw clay according to the different methods

Characteristic	Sizes	Arg1-B
Pore size (nm)	Mean diameter BJH	2.136
	Average diameter DH	2.136
	Pore width DR	6.182
	Pore diameter DA	2.92
	Pore diameter HK	1.847
	Pore diameter SF	3.46
	Pore diameter DFT	2.647

It can be seen from this table that the average pore size diameter according to the BJH and DH methods by adsorption is the same, with a good pore width calculated according to the DR method and a micro-pore diameter according to the DA method similar to that calculated by the DFT method which is the best method allowing a much more precise approach to pore size. Because it includes the size of micro-pores and narrow mesopores which other methods cannot determine. Thus, the microporous diameter size according to the HK and SF methods which take into account the pore shape, shows a considerable difference in pore size between these two methods. That of SF (3.46 nm) greatly exceeds that of HK (1.847 nm).

4. Discussion

4.1. Preliminary analyzes of raw clay (Arg1-B)

The pH obtained for this clay shows that it has surfaces which are made up of acid groups capable of reacting with the hydroxyl groups of water, which will lead to an increase in H^+ ions in the medium which is undoubtedly subject to lower the pH. The value obtained is lower than those obtained by *Zahaf*, *Bouzid* and *Qlihaa and al*, [10, 11, 13]. This difference could be due to the low alkaline and alkaline earth cation contents in these clays, which is confirmed by the results of the X-ray fluorescence analysis. The slightly low humidity rate recorded for this clay could be due to the arid character of the area where this sample was taken and shows the non-hygroscopic character of this clay, which is also confirmed by the results of the ATG-DTG. It appears from the literature that the CEC between 3 to 15 meq.100 g^{-1} corresponds to kaolinite, from 10 to 40 meq.100 g^{-1} to illite, from 80 to 150 meq.100 g^{-1} to smectites [14]. So the CEC of our determined raw clay belongs to the range of 80 to 150 meq.g^{-1}, which lets us suggest that it contains a significant amount of minerals belonging to the smectite family. The density obtained is below of that obtained by *Bouzid* [10]. This could be due to the geological formation or the experimental conditions (mesh, method) which differ, or our clay does not contain a dense element (such as quartz) likely to increase this density.

4.2. pH at the point of zero charges (pH_{PCN})

The pH_{PCN} value of the raw clay obtained in this study is almost similar to those in the literature for smectitic clays [15]. This leads us to predict that this clay still contains significant quantities of minerals belonging to the smectite family. This corroborates the hypothesis put forward above in the case of the CEC. The increase in pH_{PCN} of the clay fraction without Na^+ (Arg1-FSNa^+) would be mainly due to the elimination of certain impurities carrying positive charges which are likely to reduce this pH_{PCN} in the raw state. However, the decrease in pH_{PCN} observed in the cases of the soda clay fraction (Arg1-FNa^+) would probably be due to the adsorption of Na^+ by the negative charges of these clay fractions.

4.3. X-ray fluorescence spectrometry (XRF)

The high percentage of silica recorded could be mainly attributable to clay minerals and quartz. So this clay has a free silica content. It appears from the literature that SiO_2/Al_2O_3 ratios between 2 and 5.5 generally correspond to materials of type 2/1, more precisely montmorillonite [16, 17]. So this lets us already suggest that our clay (Arg1-B) could contain montmorillonite in large quantities. The fairly large percentage of Fe_2O_3 recorded in this raw clay could be due to the existence of minerals that can contain iron in large quantities, because according to the literature, iron is found in the form of oxide-hydroxides, namely goethite, and/or oxides such as hematite and magnetite [18, 19]. So, drawing inspiration from this result from the literature, we can say that, this clay could contain goethite and / or hematite and

magnetite. These types of minerals are generally attributable to montmorillonites. The titanium content recorded could be attributable to kaolinites, as it appears from the literature that titanium is found in the form of rutile or anatase in kaolinitic clays [8]. This leaves us to suggest that, this clay, in addition to montmorillonite, could contain kaolinite. The low percentages of CaO and MgO recorded let us predict that this clay is devoid of carbonated elements. But, the low percentage of LOI shows that it contains only a minimal amount of organic matter and carbonates.

The presence of the trace elements found (V, Cr, Ni, Zn, Cu, Ga, Sr, Y, Zr, Hf, Ba, Ce, Eu, Re and Pb) in this study differs from the results found by *Gourouza* [20] in the clays of Tahoua region in Niger, where it concludes the total absence of these elements. This could be due to the difference in the geological formations where these samples were taken.

4.4. X-ray diffraction (XRD)

In general, the XRD analysis showed that the raw clay analyzed contains a mixture of clay minerals with impurities. The main constituent minerals are montmorillonite and kaolinite and the impurities are quartz, microclines and goethite. This proves the heterogeneous nature of this clay, which is in perfect agreement with the various observations made at the SEM and the X-ray fluorescence results. It emerges from the literature that clay minerals of the kaolinitic type are always associated with impurities such as quartz and goethite, and smectitic types associated with microclines and rutile [2, 8, 10, 21]. In the soda and non-soda clay fraction, the main constituent minerals are montmorillonite and kaolinite which appear with very intense peaks, but with the persistence of certain low intensity peaks characteristic of quartz. These results are in agreement with those of several authors who reported the presence of quartz in the clay fractions [8, 13, 22]. The presence of goethite in the clay fractions of our clay is in agreement with that found by *Zaki and al*, [8] in their work in Niger in Tillaberry region. So these different observations confirm the significant elimination of quartz during the extraction of the clay fraction, these results also confirm those of X-ray fluorescence.

4.5. Thermo-gravimetric analysis

In the case of Arg1-B, the first mass loss could be attributable to the dehydration of the water adsorbed between the particles and the aggregates of this clay and those which are not directly linked to the exchangeable cations in the interlayer space. The low intensity of the peak obtained confirms the results of the moisture content, which shows that this clay does not contain a large amount of adsorbed water and this could be due to the arid nature of the area where this clay was taken. These kinds of losses in this temperature range are generally attributable to swelling clays (montmorillonite) [23]. Which is in agreement with the results of XRD and X-ray fluorescence. So this dehydration could lead to the structural reorganization of the network due to the accommodation of dehydrated cations in the hexagonal cavities of the Si-O network, which would lead to the growth of weight on the TGA curve and the appearance of the exo peak on the DTG curve or to a change in the oxidation state of these cations. The 2nd mass loss could be attributable to water dehydration linked to interfoliar cations. But, this dehydration does not lead to the structural reorganization of the network, because no growth on the ATG curve was observed after this loss. This leads us to believe that, this clay still contains significant quantities of smectitic-type minerals (montmorillonite), because according to *Villieras* [23], the dehydration of swelling clays is accompanied up to a temperature below 450°C. The 3rd and 4th ones obtained between 400 and 600°C could be attributable to the dehydroxylation of structural OH of smectitic type materials containing an appreciable amount of iron or to the dehydroxylation of Kaolinite which can be transformed into metakaolinite [24]. Which lets us predict more that, this clay could contain smectitic and kaolinitic materials. They could also be the dehydroxylation of iron-bound OH from montmorillonite. This is in agreement with the hypothesis put forward above. The latter loss could be attributable to the dehydroxylation of structural OH bound to the aluminum of montmorillonite followed by a reorganization of the structural network, which shows the weight increase on the ATG curve and the exothermic peak on the DTG curve. The well-marked exotherms imply a strong crystallinity and testify to a structural reorganization of the clay minerals by the change of the state of oxidation of the constituent elements, like the transition metals, which is in perfect agreement with the results of the fluorescence X and the observations made at the SEM.

4.6. Scanning electron microscopy

In general, the rather irregular morphologies observed on the SEM images of our clay could be largely attributable to smectitic type materials (montmorillonite) [25]. Similarly, small particles of hexagonal shape and sometimes reduced to diamonds could be attributed to kaolinites [25, 26]. The rough deposits visible on the crystals could be free silicas in this clay material and *Bellaroui and Mokhtari* impurities *in* [27]. These hypotheses are in agreement with the results of XRD, X-ray fluorescence and ATG-DTG.

4.7. Measurement of SS by the Brunauer, Emmett and Teller (BET) method

The SS obtained by the different methods except those of Langmuir, single point and DFT, do not reach that of a pure montmorillonite (880 $m^2.g^{-1}$), but largely exceed that of pure kaolinite (between 10 and 30 $m^2.g^{-1}$). These SS obtained

not reaching that of a pure montmorillonite could be due to the presence of kaolinites and impurities in these raw clays likely to attenuate the normal development of the SS of a montmorillonite. These results are in agreement with those of the DRX which showed the presence of Kaolinites and impurities in this raw clay. Similarly, the values exceeding those of kaolinite could be due to the presence of montmorillonite which could increase these SS. This is always confirmed by the results of the XRD. This leads us to suggest that this clay mainly contain montmorillonite. In addition, the values obtained in this study greatly exceed those found by many authors [1, 2, 11, 20, 22, 28]. Thus, the differences observed between the different methods, especially that of Langmuir and BET, could be attributable to the different assumptions that each of the methods is based on. The strong Langmuir SS obtained would probably be due to the three assumptions that, this model uses (the adsorption is localized and only gives rise to the formation of a monolayer; all the sites are equivalent and the surface is uniform; no interaction between adsorbed molecules). This stipulates that there is no distinction between the different pores of this clay material (micro, meso and macropore). So as this clay is made up of several types of minerals (montmorillonite and kaolinite) with impurities (goethite, quartz and other elements), this could lead to the adsorption of a large quantity of gaseous nitrogen in the various pores that this clay contains. clay, which will undoubtedly lead to the exceptional enhancement of the SS greatly exceeding that of BET. Results for Langmuir's SS for clay materials are somewhat lacking to our knowledge in the literature.

4.7.1. Pore of volume

The total pore volumes found by the methods (BJH and DH) are greater than those obtained by *Bouna* and by *Célini* [22, 28] respectively on montmorillonite, on crude and soda TAG. This could be due to the fact that our clay is made up of several minerals likely to increase the pore volume, which is confirmed by the SS obtained in this study which largely exceed those of these authors. Similarly, the microporous volume of our clay exceeds that of *Bouna* [22]. The assumption is the same as before.

4.7.2. Distribution of pore sizes

The results obtained by the different methods show that the pore sizes of our clay material are on the one hand less than 2 nm characteristic of microporous materials, and on the other hand greater than 2 nm but not reaching 50 nm characteristic of microporous materials. mesoporous materials according to the UIPCA classification. This leads us to think that, this clay could contain micro-pores and mesopores. But, according to the DFT method which gives the results of micro-pores and mesopores, shows a large peak at a diameter size of less than 2 nm confirming the presence of micro-pores and two peaks at diameter sizes greater than 2 nm confirming the presence mesopores. These hypotheses could also be confirmed by the obtained microporous SS largely exceeding that of BET. In addition, the diameter sizes obtained by the HK and SF methods and according to the pore width, let us think that this clay could contain slit-shaped micro-pores and cylindrical-shaped mesopores, because the values obtained according to these two methods are respectively less than 2 nm and greater than 2 nm. The diameter size values obtained in this study are lower than those of *Bouna* [22]. This could probably be due to the multiplicity of minerals and impurities contained in our clay on the one hand or to the large SS developed by this clay on the other.

5. Conclusion

The results of the physicochemical, mineralogical, structural and textural characterization of Tanout clay and its clay fractions show that, this clay consists of montmorillonite and kaolinite with accessory minerals such as quartz, microclines and goethite. It is also made up of trace elements (V, Cr, Ni, Zn, Cu, Ga, Sr, Y, Zr, Hf, Ba, Ce, Eu, Re and Pb) with large specific surfaces calculated according to the methods. These characteristics make this clay a good adsorbent for the elimination of polluting elements, in particular anions.

Compliance with ethical standards

Acknowledgments

Our thanks go to the heads of the Departmental Directorate of hydraulics and sanitation of Tanout, for providing us with the equipment necessary for the realization of this work.

Disclosure of conflict of interest

The authors declare that they have no competing interests

References

[1] Bouras O. Adsorbent Properties of Organophilic Bridged Clays: Synthesis and Characterization [PhD thesis]. University of Limoges, Discipline: Water Chemistry and Microbiology; 2003.

[2] Errais E. Surface reactivity of natural clays Study of the adsorption of anionic dyes [PhD thesis]. University of Strasbourg. Speciality ; Environmental Geochemistry; 2011.

[3] Gourouza M, Natatou I, Bayo K, Boos A. Study of the adsorption of fluoride ions by a bentonite from Niger. J. Soc. West-Afr. Chem. 2013; 036: 15-20.

[4] Maazou AM, Adamou R, Konaté M, Alassane A, Adel M. Valorization of two clay materials from the Niger River valley in the elimination of copper from drinking water. J. Soc. West-Afr. Chem. 2017; 043: 64 – 75.

[5] Moussa IA, Issa MSS, Hassane B, Abdourhamane TA, Garba Z, Wagani I. European Scientific Journal, ESJ. 2021; 17(3): 120-132.

[6] Hassidou S, Ahmed HH, Abdoulwaheb R, Adel M. Contribution to the Study of Useful Natural Materials from Niger: Physicochemical Characterization of Natural Nigerien Clay. J. Adv. Chem. Science. 2018; 4(3): 567–570.

[7] Marou G, Adamou Z, Ibrahim N, Anne B. Characterization of a mixed clay from Niger. Rev. CAMES – Sciences Struct. Mast. 2013; Flight. 1: 29-39.

[8] Zaki O, Abdoulaye A, Nomao DL, Rumari P, Palomino GT, Amadou I. Characterization of Soils in Irrigated Perimeters of Western Niger by X-ray Diffraction. J.Soc. West-Afr. Chem. 2008; 026: 89-97.

[9] NF P 94 050: Determination of the water content by weight of materials. Steaming method.

[10] Bouzid S. Adsorption of organic pollutants on a clay exchanged with phosphoniums. [Doctoral thesis]. University of Science and Technology of Oran Mohamed Boudiaf. Option physico-chemistry of mineral materials; 2015.

[11] Zahaf F. Structural study of modified clays applied to the adsorption of pollutants [PhD thesis]. Mustapha Stambouli University of Mascara. Speciality: Materials Chemistry; 2017.

[12] DERAFA G. Synthesis and characterization of modified montmorillonite: Application to the adsorption of cationic dyes [Memory of Magister]. University Ferhat Abbas-Setif-1-. Option: Chemical Engineering; 2014

[13] Qlihaa A, Dhimni S, Melrhaka F, SRhiri A. Physicochemical characterization of Moroccan clay. J.Mater.Environ.Sci. 2016; 7(5): 1741-1750.

[14] Abidi N. Interactions between natural clays and dyer effluents. Influence of clay surface properties and dye adsorption mechanisms [PhD thesis]. University of Strasbourg. Specialty: Geochemistry and Environment; 2015.

[15] Tombacz E, Szekeres M. Colloidal behavior of aqueous montmorillonite suspensions: the specific role of pH in the presence of indifferent electrolutes. Applied Clay Science. 2004 ; 27: 75-94.

[16] Jozja N, Baillif P, Touray JS, Pons CH, Muller F, Burgevin C. Multi-scale impacts of a (Mg, Ca)–Pb exchange and its consequences on the increase in permeability of a bentonite. Geoscience Reports. 2003; 335: 729-736.

[17] Chouchane T, Chouchane S, Boukari A. Elimination of manganese in solution by kaolin, kinetic and thermodynamic study. Journal of Renewable Energies. 2013; 16: 313-335.

[18] Sei J, Jumas JC, Olivier-Fourcade J, Quiquampoix H, Straunton S. Role of iron oxides in the phosphate adsorption properties of kaolinites from the Ivory Coast. Clays and Clay minerals. 2002; 50(2), 219–224.

[19] Soro NS, Blanchart P, Aldon L, Olivier-Fourcade J, Jumas JM, Bonnet JP. Role of Iron in Mullite Formation from Kaolins by Mössbauer Spectroscopy and Rietveld Refinement Journal of American Ceramic Society. 2003; 86 (1) 129–34.

[20] Gourouza M. Characterization of Materials (Clays, Gypsum and Calcined Bones); Quantitative, kinetic and thermodynamic study of the adsorption of fluoride ions by Sabon-Karré clay and by calcined beef bones [PhD thesis]. Abdou Moumouni University of Niamey; 2012.

[21] Zghal HB, Mhiri MMT. Physicochemical and mechanical characterization of ceramic materials obtained from Tunisian clays. Glasses, Ceramics & Composites. 2011; 1(2): 25-33.

[22] Bouna L. Functionalization of clay minerals of Moroccan origin by TiO2 for the elimination by photocatalysis of organic micropollutants from aqueous media [PhD thesis]. University of Toulouse, Discipline or specialty: Materials science and engineering; 2012.

[23] Villieras F. Study of changes in the properties of talc and chlorite by heat treatment. [Doctoral thesis]. National Polytechnic Institute of Lorraine. Geosciences-Raw Materials option; 1993.

[24] Brigatti MF. Relationship between composition and structure in Fer-rich smectites. Clay Minerals. 1983; 18: 177-186.

[25] Konan KL. Interactions between clay materials and abasic medium rich in calcium. [Doctoral thesis]. University of Limoges. Specialty: Ceramic Materials and Surface Treatments; 2006.

[26] Perrin S. Modeling the kinetics of non-isothermal and (or) non-isobaric transformations. Application to the dehydroxylation of kaolinite and to the reduction of triuranium octoxide by hydrogen [PhD thesis]. National School of Mines of Saint-Etienne. Speciality: proceeds genius; 2002.

[27] Djebbar M. Maghnia clay: purification and adsorption of pollutants. [Doctoral thesis]. University of Oran, Option: materials chemistry; 2014.

[28] Célini N. Treatment of clays by cold plasma for their use as fillers for clay-polymer nanocomposites. [Doctoral thesis] University of Maine. Specialty in chemistry and physico-chemistry of polymers; 2004.